Cuproptosis-Related lncRNAs Signature Predicts Prognosis and Chemotherapeutic Response of Patients with Lung Adenocarcinoma

Yipan Zhu
Nankai University
Huiting Deng
Nankai University
Xiuyu Wang
Nankai University
Yi Chen
Shanghai Vocational College of Agriculture and Forestry
Qiangzhe Zhang (zhangqiangzhe@nankai.edu.cn)
Nankai University

Research Article

Keywords: Cuproptosis, lncRNA, prognosis, immune infiltration, lung adenocarcinoma

Posted Date: November 10th, 2022

DOI: https://doi.org/10.21203/rs.3.rs-2239845/v1

Abstract

Cuproptosis is a lipoylated tricarboxylic acid (TCA) cycle proteins-mediated novel cell death. Long non-coding RNAs (lncRNAs) involved in multiple cell death and lung adenocarcinoma (LUAD) process and might be as a signature to predict prognosis and therapeutic response of patients. However, the predictive performance of cuproptosis-related lncRNAs (CuRLs) is still unclear in LUAD. Here, we constructed a 13-cuproptosis-related-lncRNA signature (CuRLsig) through LASSO penalized Cox regression analysis to separate patients into low- and high-risk groups. The low-risk group has longer overall survival (OS), progression-free survival (PFS) and disease-specific survival (DSS) compared to high-risk LUAD patients. The CuRLsig-derived risk score was independent of other clinical variables (age, gender, and stage) in predicting outcomes and further had better predictive ability to predict the prognosis of LUAD patients compared with other lncRNA model. Functionally, the high-risk group was associated with proteasome, spliceosome, respiratory chain and cyclin complex, p53 signaling pathway and DNA damage and repair pathways. Additionally, the CuRLsig-derived risk score can properly measure chemotherapeutic sensitivity to low- and high-risk LUAD patients. These results demonstrated that CuRLsig could be a powerful predictor and providing novel insights into the prognosis and treatment of LUAD patients.

1. Background

Lung cancer is the leading cause of cancer-related death. About 85% of lung cancer cases are non-small cell lung cancer (NSCLC), of which the most common is lung adenocarcinoma (LUAD) [1]. The occurrence of LUAD is associated with smoking, drinking, metabolic disorders, and other factors. Although inspiring advances have been obtained in clinical treatment, the survival of these patients remains relatively low [2]. One major reason is that LUAD patients are difficult to detect at early stage because of lacking powerful diagnostic biomarkers. The other reason is that these patients can't be rationally treated at advanced stage due to lacking effective prognostic biomarkers [3,4]. Therefore, it is urgent to develop efficient prognostic models to guide the treatment of LUAD patients.

Cuproptosis, a recently reported copper-dependent cell death modality, is a novel cell death pathway distinct from other forms of cell death [5–7]. Copper executes indispensable roles in various biological processes. As a cofactor of enzymes, copper is essential to physiological homeostasis, whereas excess concentration of copper can cause cytotoxicity [8]. It has been demonstrated that copper can bind directly to the lipoylated components of tricarboxylic acid (TCA) cycle, causing toxic protein stress and finally cell death [9]. Interestingly, altering intracellular copper concentration can regulate the development and progression of cancer [10–12]. Just for this reason, copper ionophores and copper chelators have been applied in anticancer treatment [13–16]. Actually, cuproptosis induction is greatly expected as a novel therapeutic approach, especially for cancers that are resistant to traditional therapeutic drugs [17,18]. Lung cancers are typically characterized by the reprogrammed TCA cycle, downregulation of energy supply through TCA cycle enable lung cancer cells to survive in nutrient-depleted or hypoxic conditions and escape from immune surveillance [19,20]. A recent study has identified several genes that are regulators of

cuproptosis. Some genes positively regulate cuproptosis, whereas others regulate negatively [21]. These cuproptosis-related genes (CuRGs) might well act as novel indictors to predict the prognosis of lung cancer.

Accumulating evidence demonstrates that lncRNAs broadly take part in many normal biological processes, such as transcriptional regulation, epigenetic regulation, and cell fate determination [22]. While lncRNAs dysfunction can induce cell apoptosis-resistance, migration and invasion, which result in cell carcinogenesis [23]. Furthermore, lncRNAs also play important roles in the progress and theranostics of lung cancer. For example, pathway crosstalk analyses have identified certain lncRNAs with gene regulatory function in LUAD [24], and some of which were showed as therapeutic targets or diagnostic markers [25]. Recently, several lncRNA-derived signatures and prognostic models have been constructed in NSCLC [24,26]. However, the big gap in this field is that cuproptosis-related lncRNAs signature (CuRLsig) for LUAD have not yet been clearly investigated.

In this study, we identified the CuRLs and further constructed a CuRLsig for LUAD patients by systematically using bioinformatics methods. Based on the CuRLsig-derived risk model, we comprehensively evaluated the biological function and prognostic performance of CuRLsig in LUAD patients. Our data highlight that CuRLsig significantly correlates with clinical prognosis and drug sensitivity, and can be a powerful prognostic biomarker for LUAD patients.

2. Results

2.1 Construction and validation of CuRLsig in LUAD patients

A total of 504 CuRLs were screened out by Pearson correlation analysis (Table S1). Thirty-six candidate prognostic CuRLs, including 10 risk factors and 26 protective factors, were identified by UCRA ($P < 0.05$, Fig. 1A). Subsequently, LASSO-penalized Cox analysis was performed to reduce the overfitting and enhance the prognostic accuracy of these CuRLs (Fig. 1B, C). Twenty-four CuRLs were selected with minimum partial likelihood deviation (Log Lambda=-3.3). Finally, 13 CuRLs significantly correlated with the OS of LUAD patients were identified out by MCRA and designated as CuRLsig (Table 1). Principally, four CuRGs, PDHB, PDHA1, LITP2 and DLST, were negatively corelated with the CuRLsig, while another four CuRGs, NLRP3, MTF1, GLS and DBT, were positively associated with the CuRLsig (Figure S2). Based on the median value of CuRLsig-derived risk score, all LUAD patients were assigned into high- and low-risk groups in training, testing and TCGA sets (Figure S3A-C). Highly mortality was found in patients from high-risk scored group than those from low-risk scored group (Figure S3D-F). The heatmap of CuRLsig expression profiles in training, testing and TCGA sets were plotted (Figure S3H-J). Notably, PCA results of CuRLsig showed that the identified CuRLsig is powerful for discriminating the high-risk patients from low-risk patients (Figure S4).

To validate the predictive performance of CuRLsig for LUAD patients, Kaplan-Meier and ROC analyses were performed. In training set of patients, lower mortality was observed in low-risk scored group than

that from high-risk scored group (median OS of 8.7 and 2.6 years, respectively; log-rank test, $P < 0.001$). The area under curves (AUC) of time-dependent ROC in training set were 0.789, 0.784 and 0.799 for 1-, 2- and 3-years OS predicted by CuRLsig, respectively (Fig. 1D). Similar results were obtained in testing and TCGA sets (Fig. 1E, F). These results support the potency of our CuRLsig on predicting the prognosis of LUAD patients.

Table 1
Cuproptosis-related lncRNA Signature

lncRNA	Coefficient	HR	HR-L (95%CI)	HR-H (95%CI)
AC138965.1	0.526050707	1.692235959	1.049704964	2.728064209
LINC02605	0.226701734	1.254455651	1.058870861	1.486167048
AC092168.2	0.185038242	1.203264455	1.066713879	1.357294938
PLUT	0.132577446	1.141767438	1.031084063	1.264332297
ARNTL2-AS1	0.113471892	1.120160403	0.987697738	1.270387975
AL161431.1	0.057111745	1.058774117	0.994621355	1.127064712
AC083806.2	-0.130710829	0.877471477	0.734977543	1.047591455
AL133445.2	-0.149653499	0.861006264	0.755743894	0.980929906
SMCR5	-0.162072817	0.85037928	0.700802791	1.031880764
AC022272.1	-0.178659912	0.836390298	0.730068157	0.958196469
AC005072.1	-0.232238534	0.792757001	0.667191902	0.941953373
LINC01447	-0.268292057	0.764684417	0.642139312	0.910615886
ADPGK-AS1	-0.308677881	0.734417302	0.585019454	0.921967243

2.2 CuRLsig was a favorable prognostic factor with excellent prediction performance in OS of LUAD patients

UCRA and MCRA were further performed to determine whether the CuRLsig could be used as an independent prognostic indicator for LUAD patients. The results showed that CuRLsig-derived risk score and tumor stage were independent of other clinical characteristics on predicting the clinical outcomes ($P < 0.05$, Fig. 2A-C). So CuRLsig is an independent OS predictor for LUAD patients. To quantify the risk of each patient, we constructed a nomogram to predict OS in 1, 3, and 5 years by weighting gender, age, stage and risk value. From the nomogram, we can find that the survival probability of a low-risk patient (patient 30) in 1-year, 3-year and 5-year is 0.958, 0.836 and 0.685, respectively (Fig. 3A). The survival probability of another high-risk patient (patient 20) in 1-year, 3-year and 5-year were 0.756, 0.311 and 0.0847, respectively (Fig. 3B). Notably, the survival of low-risk patients was much longer than that of high-risk patients. C-index curves showed that the survival prediction by risk score was much superior to that

by age, gender and stage (Fig. 3C), as well as all C-index were greater than 0.5 which reflects an good predictive performance of the nomogram. Meanwhile, the calibration plots of 1-, 3-, 5-year OS exhibited highly consistent between the actual survival rate and nomogram-predicted survival rate (Fig. 3D). Moreover, the AUCs of ROC for GIRlncSig-based risk score, age, gender and stage in TCGA set were 0.751, 0.537, 0.596 and 0.711, respectively (Fig. 3E). These results suggest that constructed nomogram possessed excellent practicable performance on OS prediction of LUAD.

To more intuitively estimate the advantage of the CuRLsig, we compared the prediction capacity of overall survival between our CuRLsig with literature-reported prognostic lncRNA models in LUAD patients. Li's prediction model was composed of 7 immune-related LncRNAs (AC022784-1, NKILA, AC026355-1, AC068338-3, LINC01843, SYNPR-AS1 and AC123595-1) [27]. In contrast, Jin's prediction model was composed of another 7 immune-related lncRNA (AC092794.1, AL034397.3, AC069023.1, AP000695.1, AC091057.1, HLA-DQB1-AS1, HSPC324) [28]. And, other 5-lncRNAs-constituted model (OGFRP1, ITGB1-DT, LMO7DN, NPSR1-AS1, PRKG1-AS1) was established by Zeng for predicting the OS of LUAD patients [29]. As shown in Fig. 3F-H, the AUCs for 1-, 2-, 3-year survival prediction by our CuRLsig were 0.751, 0.712 and 0.718, respectively. Apparently, the OS-predication performance by our CuRLsig was more sensitive than that by other three models. These results suggest that our CuRLsig-derived risk model outperformed other models in predicting the overall survival of LUAD patients.

2.3 CuRLsig possessed credible prediction performance in PFS and DSS of LUAD patients

Furthermore, we found that CuRLsig could be used as an independent PFS and DSS predictor for LUAD patients ($P < 0.05$, Fig. 4A, B). Kaplan-Meier and ROC analyses demonstrated that lower incidence rate of PFS and DSS were observed in low-risk scored group than that from high-risk scored group (Fig. 4C, D top; log-rank test, $P < 0.001$). The AUC of time-dependent ROC in TCGA set were all greater than 0.62 for PFS and DSS predicted by CuRLsig (Fig. 4C, D bottom). Moreover, the ROC results of GIRlncSig-based risk score in PFS and DSS were obviously superior to those of age, gender and stage in TCGA set (Figure S5A, B). In addition, the prediction capacities of PFS and DSS of CuRLsig were also better than those of other three models (Fig. 4E, F). These results suggest that our CuRLsig has the credible prediction performance in PFS and DSS of LUAD patients.

2.4 GIRlncSig was a stable risk model in different clinical variables of LUAD patients

To validate the stability of our model, we performed stratification analysis between risk score and clinical variables. LUAD patients were first grouped by different clinical variables, and further stratified into high- and low-risk subgroups by risk score. We found that clinicopathological variables, like survival status, Stage, T- and N-stage, and tumor relapse, were significant differences in high- and low-risk group (Figure S6A). The percentage of clinical variables in T3-4, N1-3, Stage III-IV and relapse groups were higher in high-risk subgroup than those in low-risk subgroup. As well as patients in dead, T3-4, N1-3, Stage III-IV

and relapse groups possessed higher risk scores than those in alive, T1-2, N0, stage I-II and non-relapse groups (Figure S6B-F). Kaplan-Meier survival analyses demonstrated that patients with low-risk score exhibited longer survival than those with high-risk score in all subgroups, excepting the pathologic M1-subgroup (log-rank test, $P < 0.001$; Fig. 5A-K). This may attribute to the fact that there are only 24 patients in M1-subgroup, which resulted in no survival-difference between high- and low-risk subgroups (log-rank test, $P = 0.072$; Fig. 5L). These results highlight the good stability of our GIRlncSig-based risk score model.

2.5 Biological Characteristics and Functions in Different Risk Groups

To determine the possible biological characteristics and functions in high- and low-risk groups of LUAD patients, enrichment analyses of GO, KEGG and cancer hallmark were performed using “GSVA” package. GO annotation is composed of three categories (Fig. 6A): biological process (BP), cellular component (CC) and molecular function (MF). CC results showed that the high-risk group presented enrichment of proteasome, cytochrome, respiratory chain and cyclin complex. While BP results displayed that the high-risk group enriched in redox homeostasis, mitochondrial ATP synthesis coupled electron transport and nucleic acid metabolism. Moreover, Heatmap of KEGG signaling pathways showed that proteasome, spliceosome, p53 signaling pathway and DNA damage and repair pathways were more enriched in high-risk group compared to that in low-risk group (Fig. 6B). Notably, further cancer hallmark analyses showed that the high-risk group were mainly enriched in the pathways like DNA repair, the targets of cancer genes, TNFα and MTORC1 signaling, hypoxia and glycometabolism (Fig. 6C). As the enriched biological and signal pathways are closely related to carcinogenesis process, these results suggest that the CuRLsig is essential to LUAD development.

2.6 Chemotherapeutic evaluation of LUAD patients with CuRLsig

To assess the predictive potential of CuRLsig on drug sensitivity, spearman correlation analysis was performed to estimate the IC50 of chemotherapeutics in high- and low-risk patients. A total of 65 chemotherapeutic drugs, including 5 resistance drugs and 60 sensitivity drugs, showed significant correlation with CuRLsig risk scores (Fig. 7A; Table S2**)**. Notably, Drug resistances were mainly lied in SRC/PI3K/mTOR signals inhibitors for high-risk LUAD patients such as mTOR inhibitor Rapamycin and Phenformin, SRC inhibitor KIN001-135, and PI3K inhibitor YM201636 (Fig. 7B-E). While those high-risk LUAD patients were more sensitive to receptor tyrosine kinases signals inhibitors (Fig. 7F-I), like IGF1R and IR inhibitors (BMS-754807 and GSK1904529A) and VEGFR, PDGFR, KIT inhibitors (Tivozanib and Masitinib). In addition, some metabolism (OSU-03012), DNA replication (Cisplatin, Doxorubicin, Etoposide, Methotrexate, Mitomycin C, Gemcitabine, Camptothecin), genome integrity (Talazoparib and AG-014699), and mitosis (Epothilone B, Vinorelbine, Docetaxel, Vinblastine, VX-680, Ispinesib Mesylate, Paclitaxel)signals inhibitors were more sensitive in high-risk LUAD patients than those in low-risk LUAD

patients (Figure. 7J-M). Overall, these results suggested that CuRLsig-derived score could be used for chemotherapeutic evaluation of LUAD patients.

3. Discussion

It's critical to discover predictive biomarkers to assess LUAD patients' prognosis, because LUAD is a malignancy with the high incidence and low survival rate [2]. Although various genetic abnormalities and prognostic factors have been widely recognized and developed over the years [30–32], LUAD patients still have an exceptionally high mortality rate. Except for those who are diagnosed early and receive timely treatment, the outcomes of most LUAD patients' treatment are unsatisfactory [33], and their overall prognosis is discouraging. LncRNAs were frequently used as biomarker to predict the prognosis of LUAD patients. Previous studies shown that copper-induced cell death is mediated by an ancient mechanism-protein lipoylation [9]. Compared with other types of cell death such as necrosis, apoptosis, necroptosis, pyroptosis, and ferroptosis, cuproptosis is distinct in morphology, biochemistry and genetics. Recent studies have established many biomarkers about ferroptosis that can strongly predict prognosis and antineoplastic therapy of LUAD [34,35]. Since lncRNAs played important regulation in other forms of cell death [36], they might well be also involved in the regulation of CuRGs. Therefore, identification of CuRLs has important clinical significance for predicting the prognosis of LUAD patients.

In this study, we identified 504 CuRLs and constructed a 13-CuRLs signature in LUAD patients. We looked for the correlations between CuRLs and the prognostic outcomes of LUAD patients and construct a CuRLsig-derived risk score model. Surprisingly, the CuRLsig was significantly associated with OS, PFS and DSS and accurately risk-stratifying LUAD patients. GIRlncSig-derived risk scores were significantly associated with drug sensitivity in LUAD patients. Our findings highlight that GIRlncSig-derived risk score has a good potential to predict prognosis and therapeutic response of LUAD patients.

Our new discovered CuRLsig (AC138965.1, LINC02605, AC092168.2, PLUT, ARNTL2-AS1, AL161431.1, AC083806.2, AL133445.2, SMCR5, AC022272.1, AC005072.1, LINC01447, ADPGK-AS1) are powerful indictors for survival analysis and risk stratification. The AUC values of 3-year ROC predicted by our CuRLsig were 0.799 and 0.718 for training and TCGA sets, respectively. It's worth noting that the nomogram constituted with age, gender, stage and risk score, and the prognostic performance of risk score was superior to other clinical variables (such as age, gender and stage) both in TCGA sets. Our findings were similar with another CuRLsig with seven CuRLs () in LUAD[37]. Furthermore, our CuRLsig-derived risk model significantly outperformed all previous-reported models (Li = 0.637, Jin = 0.629, Zeng = 0.679 and CuRLsig-derived score = 0.718 in TCGA set of 3-year)[27–29]. These results strong support that the identified CuRLsig are promising prognostic indicators for LUAD patients.

Exploring the CuRLsig risk score-associated biological functions and drug sensitivity can benefit to determine the new molecular characteristics of LUAD. Based on the GSVA analyses, 20 functional classes and 34 signal pathways were enriched for CuRLsig, all of which are closely associated with the

tumorigenesis[38,39]. TNFα and MTORC1 signaling, hypoxia and glycometabolism, are also mainly enriched in high-risk group[40,41]. Additionally, DNA damage and repair pathways and the targets of cancer genes are dominantly enriched in high-risk group[42]. These aspects suggested that CuRLsig-related mutation and signaling greatly contribute to the malignancy of LUAD. Further evaluation of drug sensitivity also reveals a fascinating finding. Drug resistances were mainly targeted to SRC/PI3K/mTOR signals, while chemotherapeutic sensitivities were lied in receptor tyrosine kinases signals, metabolism, DNA replication, genome integrity and mitosis signals, for high-risk LUAD patients. The above results support the predictive potential of CuRLsig for treatment response, suggesting that the risk score may be helpful to guide the use of chemotherapy and targeted therapy.

Two limitations may exist in this study. First, the discovery of CuRGs is just beginning; the prognostic model for LUAD based on current limited CuRLs may need to be updated. Second, the detailed functions of new identified CuRLs are not clear. Future works should focus on the functional validation of these novel CuRLs by experimental data.

4. Conclusion

In summary, we first constructed a novel CuRLsig consisting of thirteen CuRLs for LUAD patients. The CuRLsig-derived risk model closely correlates with clinical prognosis and therapeutic response and can be a powerful predicted biomarker for LUAD patients.

5. Material S And Methods

5.1 Data collection and processing.

The procedure of this study is outlined as the roadmap in Figure. S1. First, the transcriptome data (FPKM) and clinical information of LUAD patients were downloaded from The Cancer Genome Atlas (TCGA) databases (https://portal.gdc.cancer.gov). Then, FPKM data were transformed into TPM form, and combined with patients' survival information for analysis. Subsequently, 468 samples were obtained by eliminating normal samples and those samples with incomplete survival information. mRNA and lncRNA of these samples were annotated based on the gtf file containing gene symbol (GRCh38.p13). Finally, these samples were randomly distributed into training and testing sets at a ratio of 1:1 using "caret" package in R. The clinical information of LUAD patients was summarized (Table 2). The *P*-values of the statistics were all greater than 0.05, suggesting no grouping-induced biases existed.

Table 2
Clinical information of LUAD patients.

Covariates	Type	TCGA set (n = 468)	Testing set (n = 234)	Training set (n = 234)	*P*-value *
Age	≤ 65	224(47.86%)	113(48.29%)	111(47.44%)	0.8533
	> 65	234(50%)	115(49.15%)	119(50.85%)	
	Unknown	10(2.14%)	6(2.56%)	4(1.71%)	
Gender	FEMALE	254(54.27%)	123(52.56%)	131(55.98%)	0.5160
	MALE	214(45.73%)	111(47.44%)	103(44.02%)	
Stage	Stage I	253(54.06%)	129(55.13%)	124(52.99%)	0.8395
	Stage II	107(22.86%)	52(22.22%)	55(23.5%)	
	Stage III	75(16.03%)	34(14.53%)	41(17.52%)	
	Stage IV	25(5.34%)	13(5.56%)	12(5.13%)	
	Unknown	8(1.71%)	6(2.56%)	2(0.85%)	
T	T1	159(33.97%)	88(37.61%)	71(30.34%)	0.3440
	T2	248(52.99%)	117(50%)	131(55.98%)	
	T3	39(8.33%)	21(8.97%)	18(7.69%)	
	T4	19(4.06%)	7(2.99%)	12(5.13%)	
	TX	3(0.64%)	1(0.43%)	2(0.85%)	
M	M0	315(67.31%)	154(65.81%)	161(68.8%)	0.8407
	M1	24(5.13%)	12(5.13%)	12(5.13%)	
	MX	125(26.71%)	65(27.78%)	60(25.64%)	
	Unknown	4(0.85%)	3(1.28%)	1(0.43%)	
N	N0	302(64.53%)	149(63.68%)	153(65.38%)	0.9799
	N1	86(18.38%)	42(17.95%)	44(18.8%)	
	N2	66(14.1%)	35(14.96%)	31(13.25%)	
	N3	2(0.43%)	1(0.43%)	1(0.43%)	
	NX	11(2.35%)	6(2.56%)	5(2.14%)	
	Unknown	1(0.21%)	1(0.43%)	0(0%)	

*Chi-squared test, $P < 0.05$ means significantly different.

5.2 Identification of CuRLs.

Seventeen cuproptosis-related genes (CuRGs), NFE2L2, NLRP3, ATP7B, ATP7A, FDX1, LIAS, LIPT2, DLD, DLAT, PDHA1, PDHB, MTF1, GLS, CDKN2A, DBT, GCSH and DLST, were collected form issued literatures [8,9]. Pearson analysis was performed to determine the correlation of LUAD-related lncRNAs with CuRGs. LncRNAs correlated significantly with at least one CuRG was defined as candidate CuRLs (|Pearson correlation|>0.35 and *P*-value < 0.001). By using the "limma" package in R, expression profile of candidate CuRLs was combined with patients' survival information for screening the prognostic CuRLs.

5.3 Establishment of CuRLsig-derived risk score model.

To minimize the risk of overfitting, Cox regression analysis with a least absolute shrinkage and selection operator (LASSO) penalty was performed in training set to select the prognostic CuRLs [43,44]. First, candidate CuRLs significantly associated with the overall survival (OS) of LUAD patients were screened by univariate Cox regression analysis (UCRA) ($P < 0.01$). Then, these CuRLs were further screened by LASSO Cox regression analysis. The penalty parameter (λ) was determined by tenfold cross-validation following the minimum criteria. Finally, the CuRL-based risk score model was established as CuRLsig through multivariate Cox regression analysis (MCRA). The CuRLsig-derived risk score was calculated as follows: explncRNA1*coeflncRNA1 + explncRNA2*coeflncRNA2 + … + explncRNAi*coeflncRNAi [45,46]. Based on the median value of the risk scores, all patients were assigned into high- and low-risk groups.

5.4 Evaluation and verification of CuRLsig.

After the identification of CuRLsig in training set, its performance was validated in testing set. First, log-rank tests were used to compare the OS, progression-free survival (PFS) and disease-specific survival (DSS) of LUAD patients in high-risk groups and low-risk groups. Next, time-dependent receiver operating characteristic (ROC) curves for 1-, 2-, and 3-year survival of patients in training, testing, and TCGA sets were plotted. Then, UCRA and MCRA were performed to verify the independent prognosis of CuRLsig against routine clinical variables. Finally, prediction performance of CuRLsig and literature-reported lncRNA-signatures were compared in TCGA set [27–29] .

5.5 Construction and validation of nomogram score system.

To visualize the results of Cox regression and predict the survival of LUAD patients, the prognostic nomogram was plotted by using “rms” and “survival” packages in R software. First, Cox proportional hazards regression model was constructed by using the cph function, and the survival function was used to calculate the survival probability. Finally, nomogram function was used to create the nomogram. The concordance index (C-index) of nomogram and ROC were plotted with CuRLsig-derived risk score and clinical prognostic factors. Calibration curve analysis was used to assess the agreement between the actual and the predicted survival rates.

5.6 Principal component analysis (PCA).

PCA is an edge tool for feature-extraction and dimension-reducing of complicated data. To determine the potential differences of the gene expression profiles of patients in high- and low-risk groups, PCA were performed for the CuRLsig by employing the "scatterplot3d" package in R software [47].

5.7 Functional enrichment analysis.

Gene set variance analysis (GSVA) was conducted to investigate the biological characteristics in high- and low-risk groups based on GO, KEGG and cancer hallmark data in MSigDB database. By using the “GSVA” package in R software [48], distinct signal pathways were extracted by “limma” package with the threshold of Benjamini & Hochberg (BH) adjusted P < 0.05 and |logFC|>0.1.

5.8 Chemotherapeutic and immunotherapeutic evaluation of CuRLsig.

To predict the therapeutic performance in low- and high-risk LUAD patients, the correlation of CuRLsig-derived risk scores with chemotherapeutic and immunotherapeutic response were analyzed. The R package “pRRophetic” was employed to determine the 50% maximum inhibitory concentration (IC50) in different CuRLsig-scored groups by ridge regression. The p-value of the spearman correlation and the p-value of drug sensitivity were < 0.001 and the |Spearman Cor| was > 0.1 as the cutoff criteria. Additionally, the tumor immune fysfunction and exclusion (TIDE) tool (http://tide.dfci.harvard.edu/) was used to predict the response of immunotherapy [49]. Four scores including TIDE, microsatellite instability (MSI), T-cell exclusion and T-cell dysfunction were adopted [50].

5.9 Statistical Analysis

Student's t-test, log-rank test, Mann-Whitney U-test, chi-squared test and Wilcoxon test were used to examine the differential variables from different sets or groups. Unless noted otherwise, statistical significance in two-tailed tests was considered when $P < 0.05$. All statistical analyses were performed with R software (version 4.1.3), and visualized by functional packages.

Abbreviations

AUC
area under curve
BP
biological processes
CC
cellular components
CuRG
cuproptosis-related gene
CuRL
cuproptosis-related lncRNA
CuRLsig

cuproptosis-related lncRNAs signature
GEO
gene expression omnibus
GO
gene ontology
GSVA
gene set variance analysis
IC50
50% maximum inhibitory concentration
KEGG
kyoto encyclopedia of genes and genomes
LASSO
least absolute shrinkage and selection operator
LncRNAs
long non-coding RNA
LUAD
lung adenocarcinoma
MCRA
multivariate Cox regression analysis
MF
molecular functions
MSI
microsatellite instability
NSCLC
non-small cell lung cancer
OS
overall survival
ROC
receiver operating characteristic curve
ssGSEA
single-sample gene set enrichment analysis
TCGA
the cancer genomeatlas
UCRA
univariate Cox regression analysis.

Declarations

Ethics approval and consent to participate

Ethnical is not applicable because these data are from the public database.

Consent for publication

All authors approved the final version of this manuscript for publication.

Availability of data and material

All the data generated and analyzed during this study are included in the manuscript and the additional materials.

Competing interests

The authors declare that they have no competing interests.

Funding

This work was supported by the National Natural Science Foundation of China (No. 82073233), the Natural Science Foundation of Tianjin (NO. 20JCQNJC00960 and 21JCQNJC00130), Science and Technology Talents Development program of Tianjin Health Commission (NO. KJ20129).

Authors' contributions

Q Z, Y C, H D initiated the idea, designed the experiments, Q Z, Y C supervised the research, P Z wrote the manuscript. P Z, H D, Q Z and X W collected, analyzed and generated data and figures. All authors have read, edited and approved the final version of this manuscript.

Acknowledgements

We are very grateful to Professor Sihe Zhang (School of Medicine, Nankai University) for his help and advice on English revision of this manuscript.

References

1. Sung H, Ferlay J, Siegel RL, et al. Global Cancer Statistics 2020: GLOBOCAN Estimates of Incidence and Mortality Worldwide for 36 Cancers in 185 Countries. *CA: a cancer journal for clinicians*. May 2021;71(3):209-249. https://doi.org10.3322/caac.21660.
2. Siegel RL, Miller KD, Fuchs HE, Jemal A. Cancer statistics, 2022. *CA: a cancer journal for clinicians*. Jan 2022;72(1):7-33. https://doi.org10.3322/caac.21708.
3. Mao Y, Yang D, He J, Krasna MJ. Epidemiology of Lung Cancer. *Surgical oncology clinics of North America*. Jul 2016;25(3):439-45. https://doi.org10.1016/j.soc.2016.02.001.
4. Puri T. Targeted therapy in nonsmall cell lung cancer. *Indian journal of cancer*. Jan-Mar 2017;54(1):83-88. https://doi.org10.4103/ijc.IJC_258_17.
5. Tang D, Kang R, Berghe TV, Vandenabeele P, Kroemer G. The molecular machinery of regulated cell death. *Cell research*. May 2019;29(5):347-364. https://doi.org10.1038/s41422-019-0164-5.

6. Wang Y, Zhang L, Zhou F. Cuproptosis: a new form of programmed cell death. *Cellular & molecular immunology*. Apr 22 2022. https://doi.org10.1038/s41423-022-00866-1.
7. Tang D, Chen X, Kroemer G. Cuproptosis: a copper-triggered modality of mitochondrial cell death. *Cell research*. May 2022;32(5):417-418. https://doi.org10.1038/s41422-022-00653-7.
8. Ge EJ, Bush AI, Casini A, et al. Connecting copper and cancer: from transition metal signalling to metalloplasia. *Nature reviews Cancer*. Feb 2022;22(2):102-113. https://doi.org10.1038/s41568-021-00417-2.
9. Tsvetkov P, Coy S, Petrova B, et al. Copper induces cell death by targeting lipoylated TCA cycle proteins. *Science (New York, NY)*. Mar 18 2022;375(6586):1254-1261. https://doi.org10.1126/science.abf0529.
10. Babak MV, Ahn D. Modulation of Intracellular Copper Levels as the Mechanism of Action of Anticancer Copper Complexes: Clinical Relevance. *Biomedicines*. Jul 21 2021;9(8). https://doi.org10.3390/biomedicines9080852.
11. Cui L, Gouw AM, LaGory EL, et al. Mitochondrial copper depletion suppresses triple-negative breast cancer in mice. *Nature biotechnology*. Mar 2021;39(3):357-367. https://doi.org10.1038/s41587-020-0707-9.
12. Tsang T, Posimo JM, Gudiel AA, Cicchini M, Feldser DM, Brady DC. Copper is an essential regulator of the autophagic kinases ULK1/2 to drive lung adenocarcinoma. *Nature cell biology*. Apr 2020;22(4):412-424. https://doi.org10.1038/s41556-020-0481-4.
13. Brady DC, Crowe MS, Greenberg DN, Counter CM. Copper Chelation Inhibits BRAF(V600E)-Driven Melanomagenesis and Counters Resistance to BRAF(V600E) and MEK1/2 Inhibitors. *Cancer research*. Nov 15 2017;77(22):6240-6252. https://doi.org10.1158/0008-5472.Can-16-1190.
14. Davis CI, Gu X, Kiefer RM, Ralle M, Gade TP, Brady DC. Altered copper homeostasis underlies sensitivity of hepatocellular carcinoma to copper chelation. *Metallomics : integrated biometal science*. Dec 23 2020;12(12):1995-2008. https://doi.org10.1039/d0mt00156b.
15. Chen D, Cui QC, Yang H, Dou QP. Disulfiram, a clinically used anti-alcoholism drug and copper-binding agent, induces apoptotic cell death in breast cancer cultures and xenografts via inhibition of the proteasome activity. *Cancer research*. Nov 1 2006;66(21):10425-33. https://doi.org10.1158/0008-5472.can-06-2126.
16. O'Day SJ, Eggermont AM, Chiarion-Sileni V, et al. Final results of phase III SYMMETRY study: randomized, double-blind trial of elesclomol plus paclitaxel versus paclitaxel alone as treatment for chemotherapy-naive patients with advanced melanoma. *Journal of clinical oncology : official journal of the American Society of Clinical Oncology*. Mar 20 2013;31(9):1211-8. https://doi.org10.1200/jco.2012.44.5585.
17. Cobine PA, Brady DC. Cuproptosis: Cellular and molecular mechanisms underlying copper-induced cell death. *Molecular cell*. May 19 2022;82(10):1786-1787. https://doi.org10.1016/j.molcel.2022.05.001.

18. Li SR, Bu LL, Cai L. Cuproptosis: lipoylated TCA cycle proteins-mediated novel cell death pathway. *Signal transduction and targeted therapy*. May 13 2022;7(1):158. https://doi.org10.1038/s41392-022-01014-x.
19. Hensley CT, Faubert B, Yuan Q, et al. Metabolic Heterogeneity in Human Lung Tumors. *Cell*. Feb 11 2016;164(4):681-94. https://doi.org10.1016/j.cell.2015.12.034.
20. Faubert B, Li KY, Cai L, et al. Lactate Metabolism in Human Lung Tumors. *Cell*. Oct 5 2017;171(2):358-371 e9. https://doi.org10.1016/j.cell.2017.09.019.
21. Bian Z, Fan R, Xie L. A Novel Cuproptosis-Related Prognostic Gene Signature and Validation of Differential Expression in Clear Cell Renal Cell Carcinoma. *Genes*. May 10 2022;13(5). https://doi.org10.3390/genes13050851.
22. Lee JT. Epigenetic regulation by long noncoding RNAs. *Science (New York, NY)*. Dec 14 2012;338(6113):1435-9. https://doi.org10.1126/science.1231776.
23. Zhao M, Feng J, Tang L. Competing endogenous RNAs in lung cancer. *Cancer biology & medicine*. Feb 15 2021;18(1):1-20. https://doi.org10.20892/j.issn.2095-3941.2020.0203.
24. Lu T, Wang Y, Chen D, Liu J, Jiao W. Potential clinical application of lncRNAs in non-small cell lung cancer. *OncoTargets and therapy*. 2018;11:8045-8052. https://doi.org10.2147/ott.S178431.
25. Peng W, Wang J, Shan B, et al. Diagnostic and Prognostic Potential of Circulating Long Non-Coding RNAs in Non Small Cell Lung Cancer. *Cellular physiology and biochemistry : international journal of experimental cellular physiology, biochemistry, and pharmacology*. 2018;49(2):816-827. https://doi.org10.1159/000493043.
26. Luo D, Deng B, Weng M, Luo Z, Nie X. A prognostic 4-lncRNA expression signature for lung squamous cell carcinoma. *Artificial cells, nanomedicine, and biotechnology*. Sep 2018;46(6):1207-1214. https://doi.org10.1080/21691401.2017.1366334.
27. Li JP, Li R, Liu X, et al. A Seven Immune-Related lncRNAs Model to Increase the Predicted Value of Lung Adenocarcinoma. *Frontiers in oncology*. 2020;10:560779. https://doi.org10.3389/fonc.2020.560779.
28. Jin D, Song Y, Chen Y, Zhang P. Identification of a Seven-lncRNA Immune Risk Signature and Construction of a Predictive Nomogram for Lung Adenocarcinoma. *BioMed research international*. 2020;2020:7929132. https://doi.org10.1155/2020/7929132.
29. Zeng L, Wang W, Chen Y, et al. A five-long non-coding RNA signature with the ability to predict overall survival of patients with lung adenocarcinoma. *Experimental and therapeutic medicine*. Dec 2019;18(6):4852-4864. https://doi.org10.3892/etm.2019.8138.
30. Wu Q, Wang L, Wei H, et al. Integration of multiple key molecules in lung adenocarcinoma identifies prognostic and immunotherapeutic relevant gene signatures. *International immunopharmacology*. Jun 2020;83:106477. https://doi.org10.1016/j.intimp.2020.106477.
31. Zhao Y, Wang R, Shen X, et al. Minor Components of Micropapillary and Solid Subtypes in Lung Adenocarcinoma are Predictors of Lymph Node Metastasis and Poor Prognosis. *Annals of surgical oncology*. Jun 2016;23(6):2099-105. https://doi.org10.1245/s10434-015-5043-9.

32. Fujimoto J, Nunomura-Nakamura S, Liu Y, et al. Development of Kras mutant lung adenocarcinoma in mice with knockout of the airway lineage-specific gene Gprc5a. *International journal of cancer*. Oct 15 2017;141(8):1589-1599. https://doi.org10.1002/ijc.30851.
33. Wang J, Wang Y, Tong M, Pan H, Li D. Research progress of the clinicopathologic features of lung adenosquamous carcinoma. *OncoTargets and therapy*. 2018;11:7011-7017. https://doi.org10.2147/ott.S179904.
34. Liu Y, Zhang X, Zhang J, Tan J, Li J, Song Z. Development and Validation of a Combined Ferroptosis and Immune Prognostic Classifier for Hepatocellular Carcinoma. *Frontiers in cell and developmental biology*. 2020;8:596679. https://doi.org10.3389/fcell.2020.596679.
35. Zhuo S, Chen Z, Yang Y, Zhang J, Tang J, Yang K. Clinical and Biological Significances of a Ferroptosis-Related Gene Signature in Glioma. *Frontiers in oncology*. 2020;10:590861. https://doi.org10.3389/fonc.2020.590861.
36. Fu XZ, Zhang XY, Qiu JY, et al. Whole-transcriptome RNA sequencing reveals the global molecular responses and ceRNA regulatory network of mRNAs, lncRNAs, miRNAs and circRNAs in response to copper toxicity in Ziyang Xiangcheng (Citrus junos Sieb. Ex Tanaka). *BMC plant biology*. Nov 21 2019;19(1):509. https://doi.org10.1186/s12870-019-2087-1.
37. Mo X, Hu D, Yang P, et al. A novel cuproptosis-related prognostic lncRNA signature and lncRNA MIR31HG/miR-193a-3p/TNFRSF21 regulatory axis in lung adenocarcinoma. *Frontiers in oncology*. 2022;12:927706. https://doi.org10.3389/fonc.2022.927706.
38. Xu K, Liu P, Wei W. mTOR signaling in tumorigenesis. *Biochim Biophys Acta*. Dec 2014;1846(2):638-54. https://doi.org10.1016/j.bbcan.2014.10.007.
39. Oshima H, Ishikawa T, Yoshida GJ, et al. TNF-alpha/TNFR1 signaling promotes gastric tumorigenesis through induction of Noxo1 and Gna14 in tumor cells. *Oncogene*. Jul 17 2014;33(29):3820-9. https://doi.org10.1038/onc.2013.356.
40. Gomez CR. Editorial: Tumor Hypoxia: Impact in Tumorigenesis, Diagnosis, Prognosis, and Therapeutics. *Frontiers in oncology*. 2016;6:229. https://doi.org10.3389/fonc.2016.00229.
41. Peng Y, Yang H, Li S. The role of glycometabolic plasticity in cancer. *Pathol Res Pract*. Oct 2021;226:153595. https://doi.org10.1016/j.prp.2021.153595.
42. de Almeida LC, Calil FA, Machado-Neto JA, Costa-Lotufo LV. DNA damaging agents and DNA repair: From carcinogenesis to cancer therapy. *Cancer Genet*. Apr 2021;252-253:6-24. https://doi.org10.1016/j.cancergen.2020.12.002.
43. Simon N, Friedman J, Hastie T, Tibshirani R. Regularization Paths for Cox's Proportional Hazards Model via Coordinate Descent. *Journal of statistical software*. Mar 2011;39(5):1-13. https://doi.org10.18637/jss.v039.i05.
44. Zhang X, Lu N, Wang L, et al. Recent advances of m(6)A methylation modification in esophageal squamous cell carcinoma. *Cancer Cell Int*. Aug 10 2021;21(1):421. https://doi.org10.1186/s12935-021-02132-2.

45. Chen SH, Lin F, Zhu JM, et al. An immune-related lncRNA prognostic model in papillary renal cell carcinoma: A lncRNA expression analysis. *Genomics*. Jan 2021;113(1 Pt 2):531-540. https://doi.org10.1016/j.ygeno.2020.09.046.
46. Li X, Meng Y. Survival analysis of immune-related lncRNA in low-grade glioma. *BMC cancer*. Aug 16 2019;19(1):813. https://doi.org10.1186/s12885-019-6032-3.
47. Schmidt P, Hörmansdörfer C, Oehler K, Härtel H, Hillemanns P, Scharf A. [Three-dimensional scatter plot analysis to estimate the risk of foetal aneuloidy]. *Zeitschrift fur Geburtshilfe und Neonatologie*. Aug 2008;212(4):127-35. https://doi.org10.1055/s-2008-1004708.
48. Hänzelmann S, Castelo R, Guinney J. GSVA: gene set variation analysis for microarray and RNA-seq data. *BMC bioinformatics*. Jan 16 2013;14:7. https://doi.org10.1186/1471-2105-14-7.
49. Parikh ND. PRO: Hepatocellular Carcinoma Surveillance: A Useful Tool Against the Rising Tide of HCC. *The American journal of gastroenterology*. Nov 2017;112(11):1632-1633. https://doi.org10.1038/ajg.2017.366.
50. Zeng Z, Li J, Zhang J, et al. Immune and stromal scoring system associated with tumor microenvironment and prognosis: a gene-based multi-cancer analysis. *J Transl Med*. Aug 3 2021;19(1):330. https://doi.org10.1186/s12967-021-03002-1.

Figures

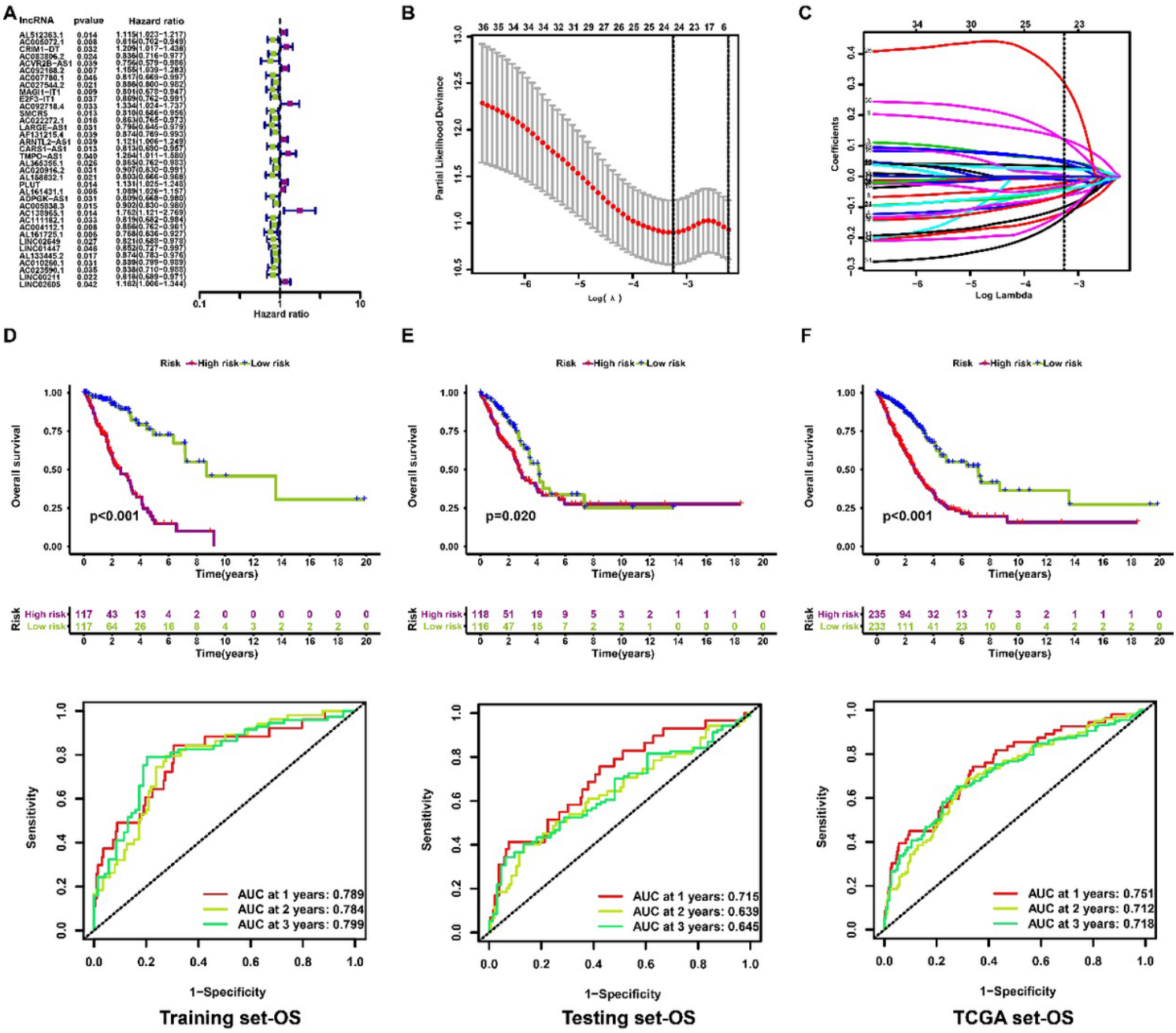

Figure 1

Construction and validationof CuRLsig for LUAD patients. (A) Forest plot of prognostic CuRLs identified by UCRA. **(B)** Distribution plot of partial likelihood based on the LASSO regression analysis. Twenty-four CuRLs were selected when Log Lambda was equal to -3.3 (the minimum). **(C)** Distribution plot of LASSO coefficient curve (Log Lambda=-3.3). **(D-F)** Kaplan-Meier OS curves (top; log-rank test, *P*<0.05) and 1-,2-,3-year ROC curves (bottom) of CuRLsig-derived low- and high-risk LUAD patients in training (D), testing (E), and TCGA (F) sets.

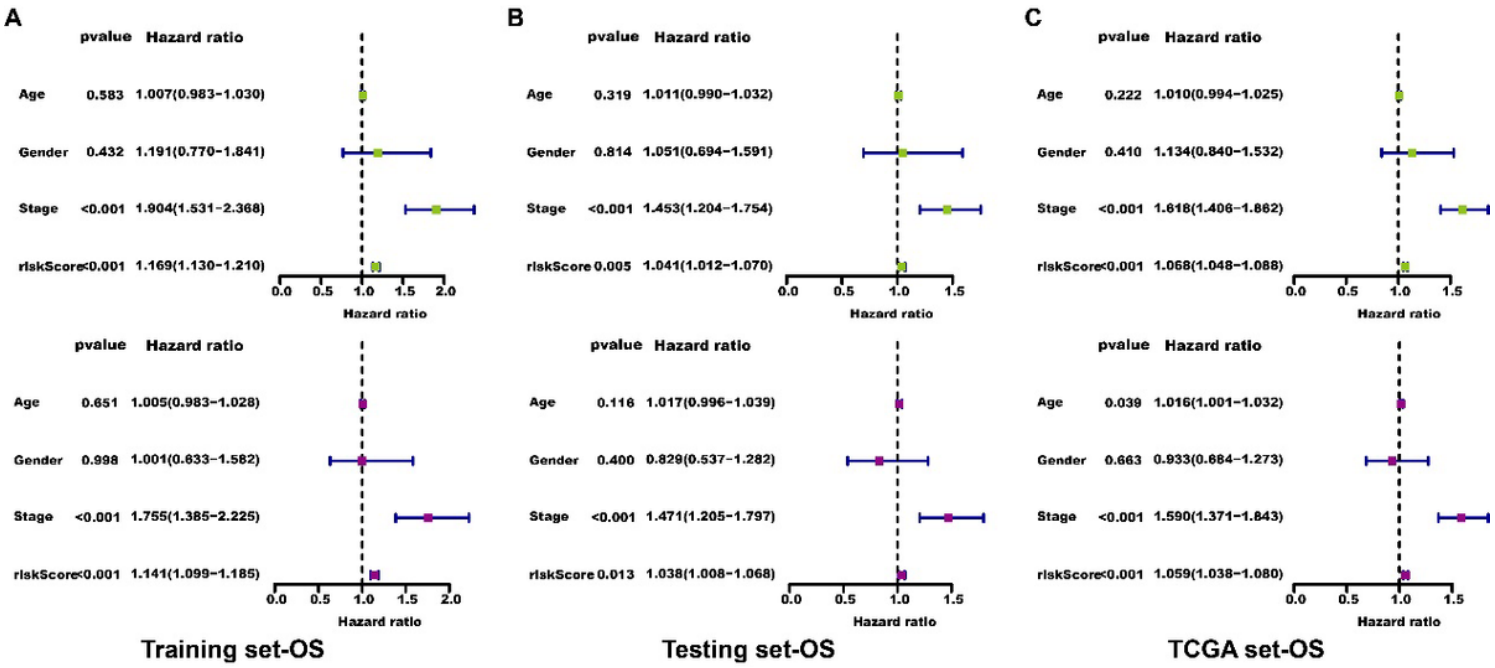

Figure 2

Independent prognostic analysis of CuRLsig for LUAD patients. Cox regression analysis of CuRLsig-derived risk score with clinical variables in training set-OS (**A**), testing set-OS (**B**), TCGA set-OS (**C**). Green represents UCRA (top), and purple represents MCRA (bottom).

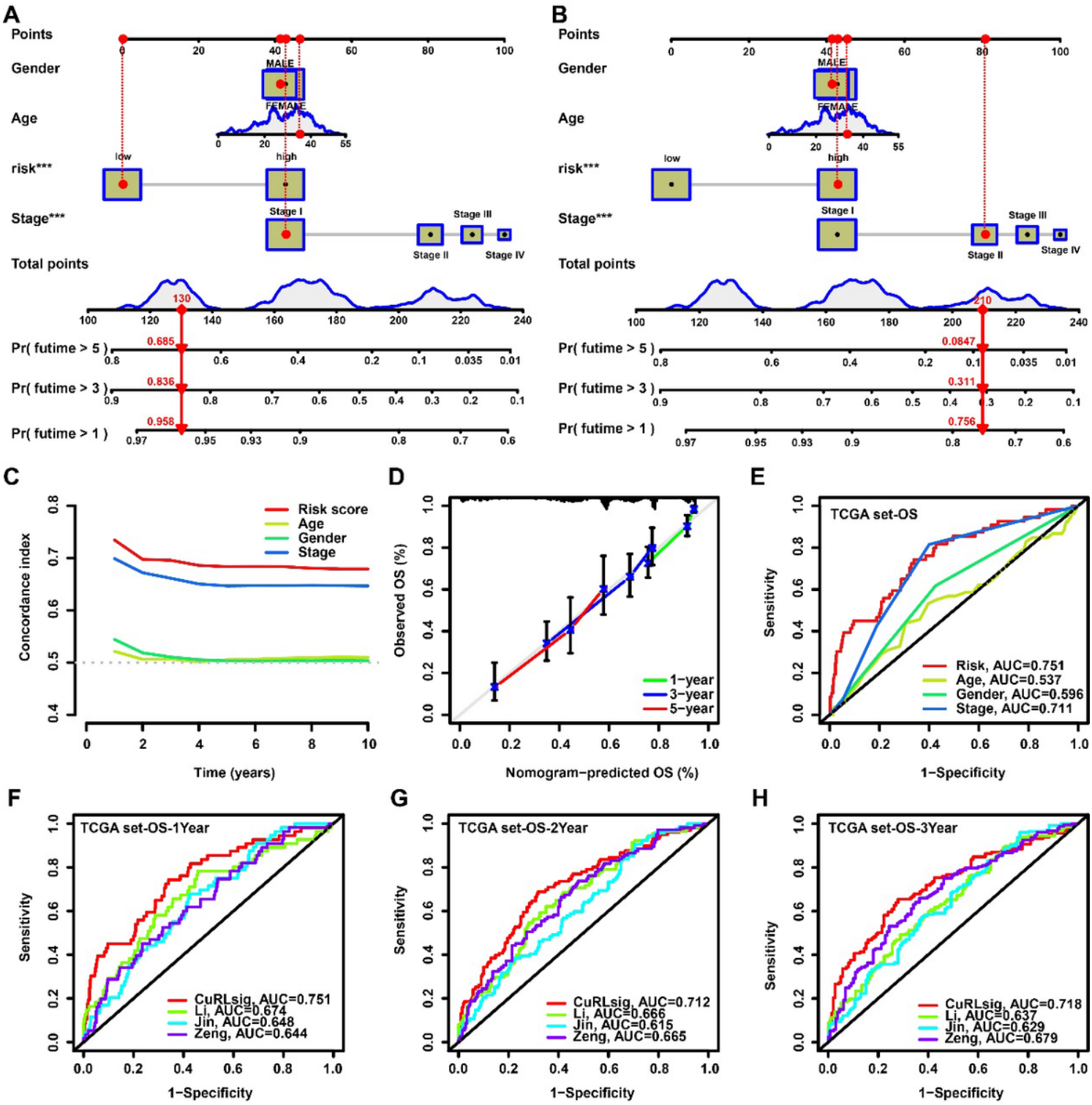

Figure 3

Nomogram construction and evaluation of CuRLsig for LUAD patients.

(A-B) Nomogram construction for predicting 1-, 3-, and 5-year OS of LUAD patients in low-risk group (A) and high-risk group (B). **(C)** C-index curves of CuRLsig-derived risk score and clinical variables. **(D)** Calibration curves analysis for the 1-, 3- and 5- year OS of LUAD patients. **(E)** ROC of CuRLsig-derived risk

score and clinical variables for TCGA set-OS. **(F-H)** The area under ROC curves of 1- (F), 2- (G), and 3-year (H) OS between our CuRLsig and other prognostic lncRNA signatures.

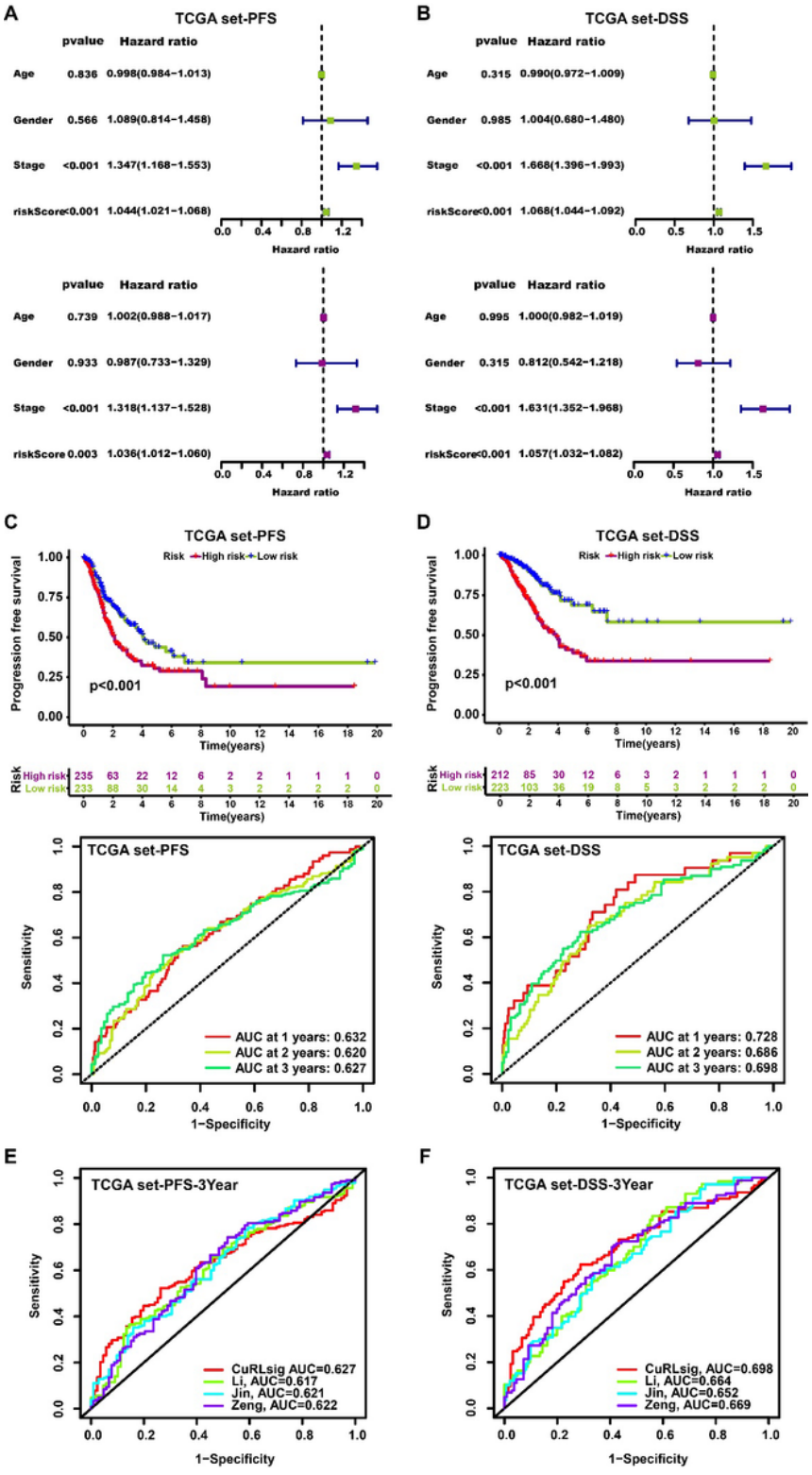

Figure 4

Independent prognostic analysis and evaluation of CuRLsig in PFS and DSS of LUAD patients. UCRA and MCRA of CuRLsig-derived risk score with clinical variables in PFS (**A**) and DSS (**B**) of LUAD patients.

Green represents UCRA (top), and purple represents MCRA (bottom). **(C, D)** Kaplan-Meier curves (top; log-rank test, *P*<0.001) and 1-,2-,3-year ROC curves (bottom) of CuRLsig-derived low- and high-risk LUAD patients in PFS (C) and DSS (D) assay. **(E, F)** The area under ROC curves of 3-year PFS (E) and DSS (F) between our CuRLsig and other prognostic lncRNA signatures.

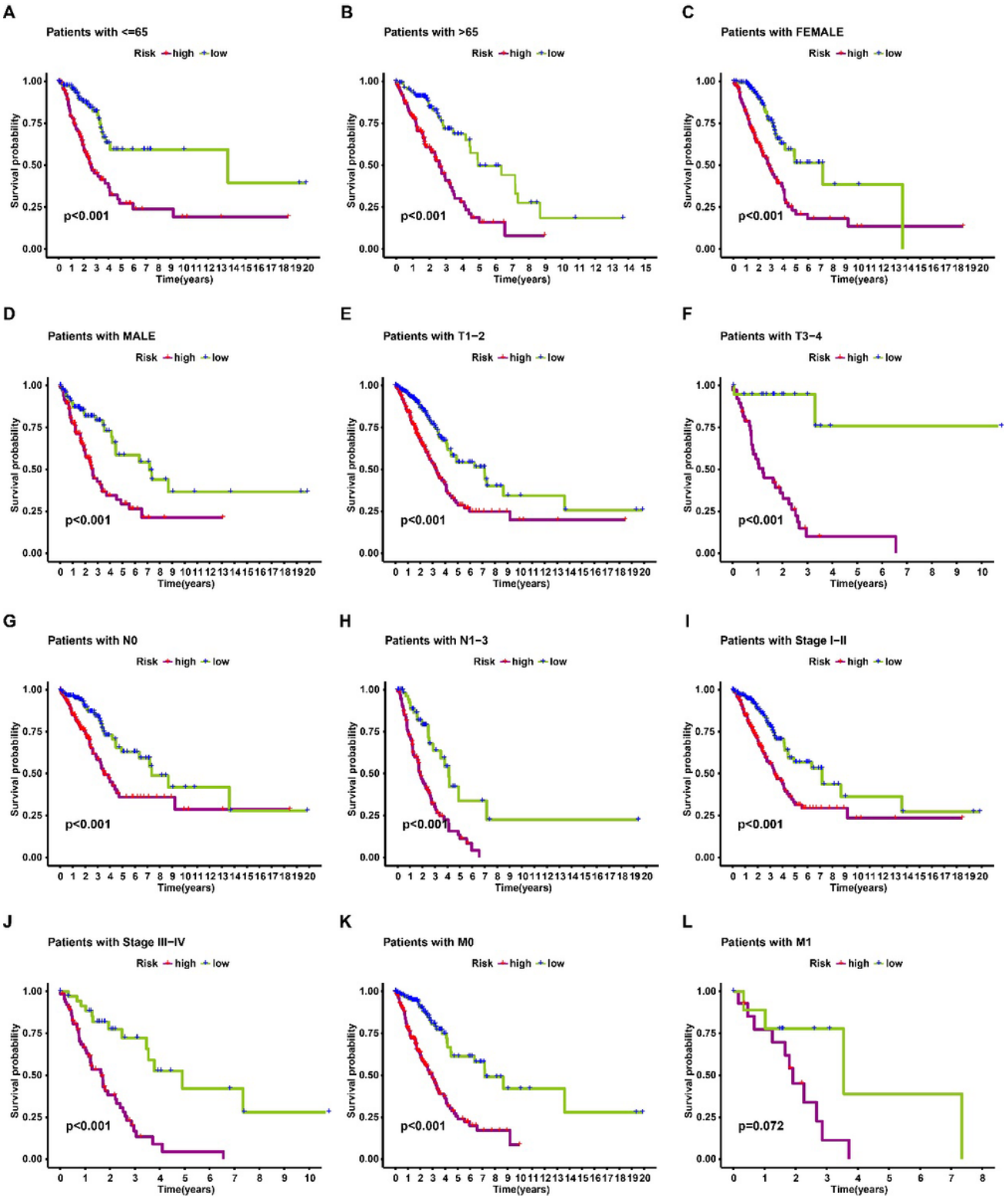

Figure 5

Stratification analyses between CuRLsig-derived risk scores and clinical variables. These clinical variables included (**A-B**) Age (≤65 vs >65), (**C-D**) gender (female vs male), (**E-F**) T-stage (T1-2 vs T3-4), (**G-H**) N-stage (N0 vs N1-3), (**I-J**) Stage (Stage I-II vs Stage III-IV) and (**K-L**) M-stage (M0 vs M1). T: tumor, N: nodal, M: metastasis.

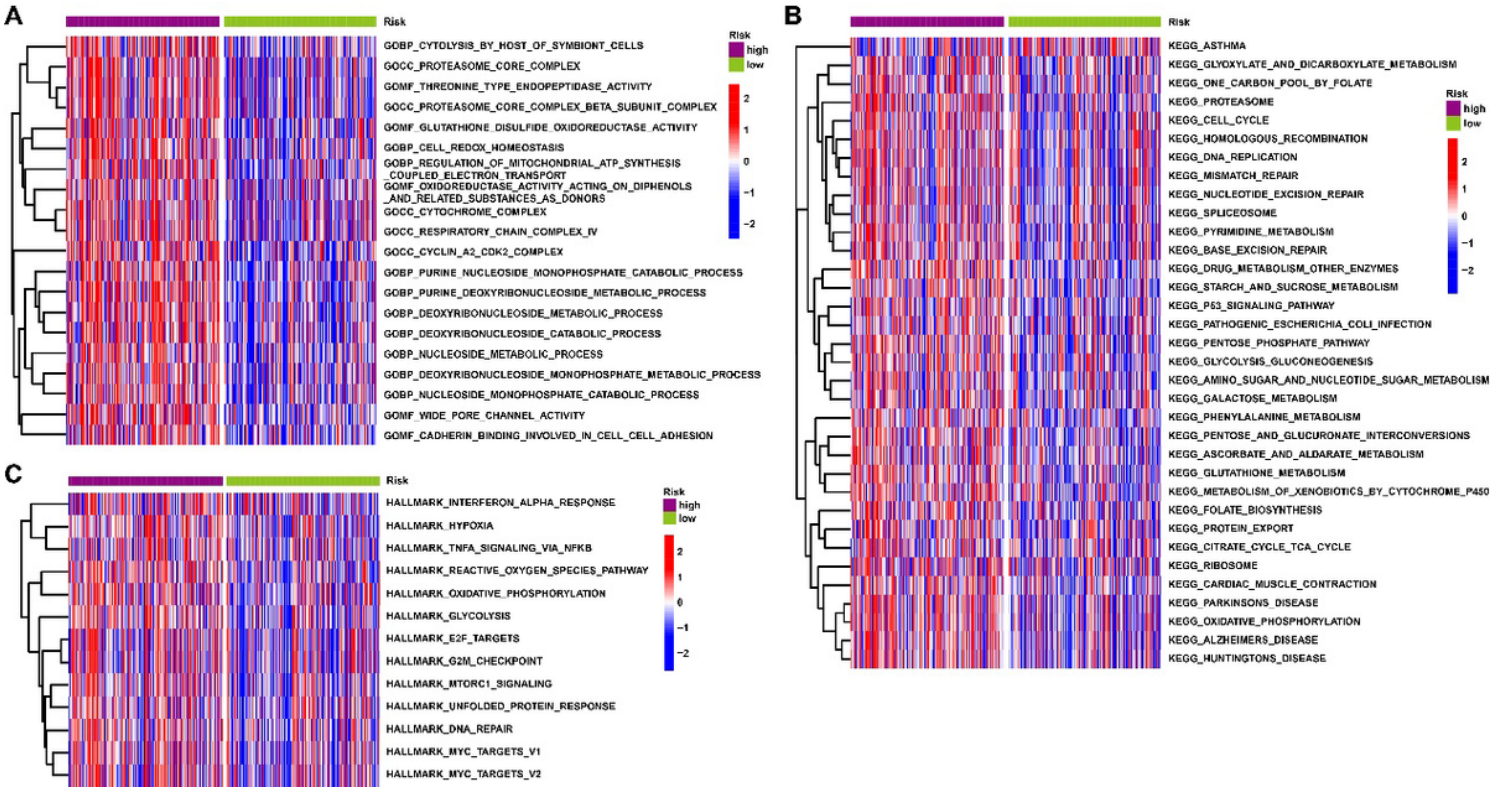

Figure 6

Functions and pathway enrichment analyses in high- and low-risk groups. (A) Heatmap of the GO enrichment analysis in low- and high-risk groups using “GSVA” package. **(B-C)** GSVA analysis for KEGG pathway (B) and cancer hallmark (C) in low- and high-risk groups.

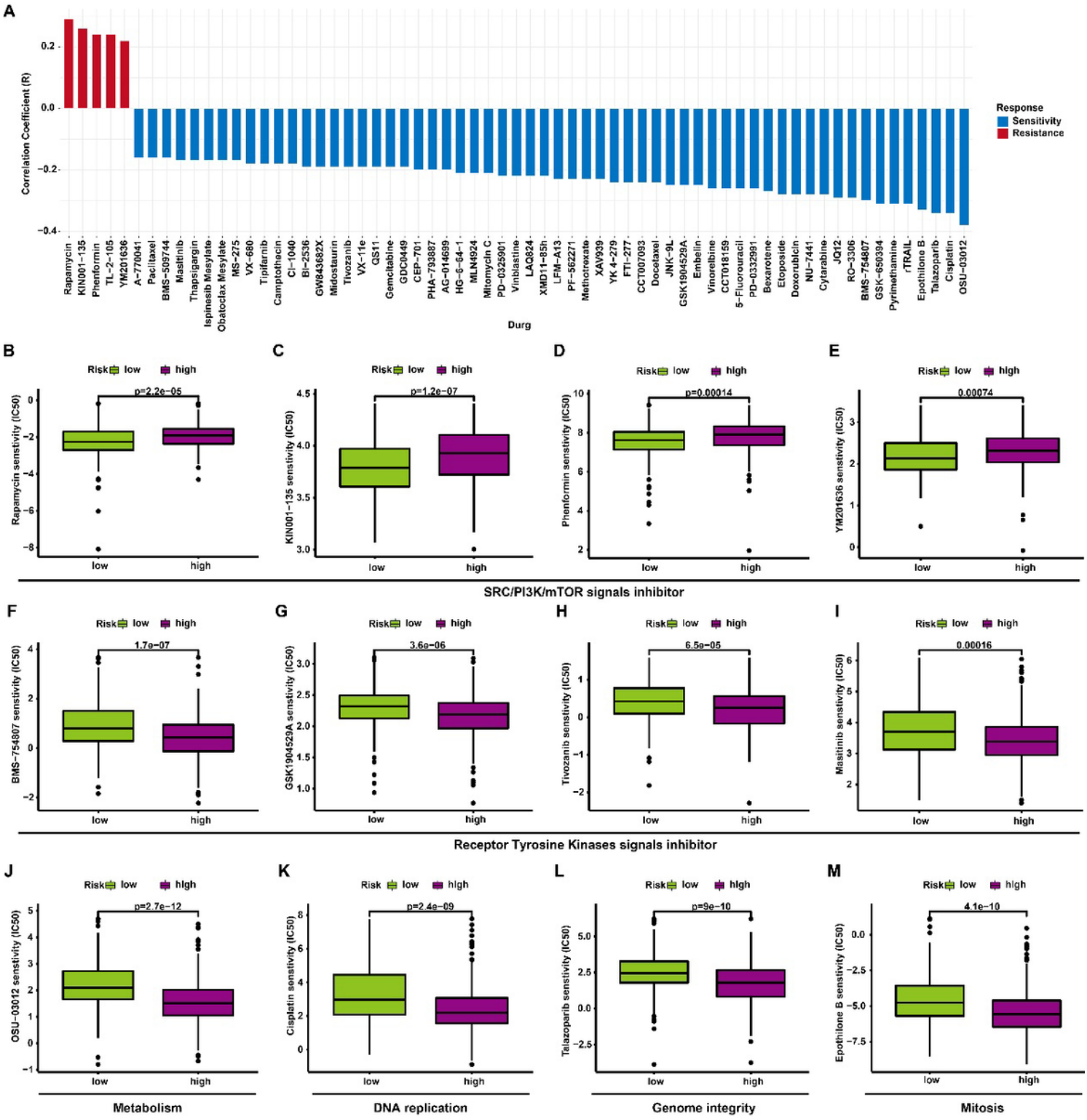

Figure 7

Chemotherapeutic responses in high- and low-risk groups patients with LUAD.

(**A**) Chemotherapeuticsensitivity and resistance for high- and low-risk LUADpatients by pRRophetic analysis. **(B-E)** Drug resistance for SRC/PI3K/mTOR signals inhibitor in high-risk LUAD patients such as (B) Rapamycin (mTOR inhibitor), (C) KIN001-135 (SRC inhibitor), (D) Phenformin (mTOR inhibitor) and (E) YM201636 (PI3K inhibitor). **(F-I)** Chemotherapeutic sensitivity for receptor tyrosine kinases signals

inhibitor in high-risk LUAD patients such as (F) BMS-754807 (IGF1R and IR inhibitor), (G) GSK1904529A (IGF1R and IR inhibitor), (H) Tivozanib (VEGFR, PDGFR, KIT inhibitor) and (I) Masitinib (PDGFR, KIT inhibitor). **(J-M)** Drugsensitivity for metabolism, DNA replication, genome integrity, and mitosis signals inhibitor in high-risk LUADpatients such as (J) OSU-03012, (K) Cisplatin, (L) Talazoparib and (M) Epothilone B.

Supplementary Files

This is a list of supplementary files associated with this preprint. Click to download.

- ZhuetalBEOsupplementaryfileacceptedchanges.docx